Variable HIV peptide stability in human cytosol is critical to epitope presentation and immune escape

Estibaliz Lazaro,[1] Carl Kadie,[2] Pamela Stamegna,[1] Shao Chong Zhang,[1] Pauline Gourdain,[1] Nicole Y. Lai,[1] Mei Zhang,[1] Sergio A. Martinez,[1] David Heckerman,[3] and Sylvie Le Gall[1]

[1]Ragon Institute of MGH, MIT and Harvard, Massachusetts General Hospital and Harvard Medical School, Boston, Massachusetts, USA.
[2]eScience Research Group, Microsoft Research, Redmond, Washington, USA. [3]eScience Research Group, Microsoft Research, Los Angeles, California, USA.

Induction of virus-specific CD8^{+} T cell responses is critical for the success of vaccines against chronic viral infections. Despite the large number of potential MHC-I–restricted epitopes located in viral proteins, MHC-I–restricted epitope generation is inefficient, and factors defining the production and presentation of MHC-I–restricted viral epitopes are poorly understood. Here, we have demonstrated that the half-lives of HIV-derived peptides in cytosol from primary human cells were highly variable and sequence dependent, and significantly affected the efficiency of cell recognition by CD8^{+} T cells. Furthermore, multiple clinical isolates of HLA-associated HIV epitope variants displayed reduced half-lives relative to consensus sequence. This decreased cytosolic peptide stability diminished epitope presentation and CTL recognition, illustrating a mechanism of immune escape. Chaperone complexes including Hsp90 and histone deacetylase HDAC6 enhanced peptide stability by transient protection from peptidase degradation. Based on empirical results with 166 peptides, we developed a computational approach utilizing a sequence-based algorithm to estimate the cytosolic stability of antigenic peptides. Our results identify sequence motifs able to alter the amount of peptide available for loading onto MHC-I, suggesting potential new strategies to modulate epitope production from vaccine immunogens.

Introduction

Despite the large number of potential MHC-I–restricted epitopes located in viral proteins, the number of virus-specific CD8^{+} T cell immune responses elicited during infection is limited. Although a comprehensive identification of MHC-bound epitopes remains limited by technological hurdles, the relative paucity of antigenic peptides likely reflects the inefficiency of epitope production. According to calculations based on protein synthesis and degradation rates occurring in a mouse cell line, it is estimated that 300–5,000 ovalbumin polypeptides are required to generate one MHC-I–epitope complex (1). Little is known about the causes of this inefficiency, though methods to enhance epitope production may be immediately applicable for vaccine design.

Endogenous proteins and defective ribosomal products are degraded in the cytosol by proteasomes into small fragments of 2–32 aa in length that can be further shortened by aminopeptidases and endopeptidases. Peptides of at least 8 residues with appropriate anchor residues are translocated by the transporter associated with antigen processing (TAP) complex into the ER, where they can be further trimmed by ER-resident aminopeptidases (ERAP1 or ERAP2) and, provided that they incorporate appropriate anchor residues, loaded onto MHC-I (2).

Oligopeptides produced during protein degradation can be subjected to cleavage in the cytosol (3, 4) by one or multiple peptidases such as thimet oligopeptidase (TOP) (5, 6) and tripeptidyl peptidase II (TPPII) (7, 8), thus limiting the amount of peptides available for MHC-I presentation. Microinjection

of fluorescent peptides into immortalized cells revealed an intracellular half-life of less than 30 seconds of various oligopeptides of fewer than 12 aa (3, 9). The degradation rate of peptides containing charged residues at positions 1 and 2 was reduced compared with that of peptides with hydrophobic residues (3), and it has been proposed that aggregation of an influenza virus peptide (PA$_{224-233}$) in pools may slow down degradation and favor rapid cross-presentation (4). However, the mechanisms underlying peptide sensitivity to degradation, their potential impact on epitope presentation, and subsequent recognition of cells by virus-specific CTLs are unknown. Research on HIV has generated extensive data on HLA-restricted epitopes and CTL responses, thereby providing an excellent model to identify factors driving the production of antigenic peptides and to assess the impact of intracellular peptide stability on epitope presentation and recognition by CD8^{+} T cells.

Here we show that the cytosolic stability rates of 8- to 11-aa-long optimally defined HIV-derived peptides are highly variable, with some being unusually stable. Intracellular stability was associated with specific motifs located throughout the peptide sequences. Furthermore, we established a computational model to assess intracellular stability of short peptides. We observed that degradation of peptides was performed by multiple peptidases and that enhanced peptide stability could be mediated through protection by chaperone complexes. Finally, multiple HLA-associated mutations occurring within HIV epitopes dramatically decreased the intracellular stability of peptides. Higher sensitivity to cytosolic degradation reduced the amount of peptides displayed at the cell surface and hindered recognition by CTLs, thus constituting what we believe to be a novel mechanism of immune escape. These results identify a critical
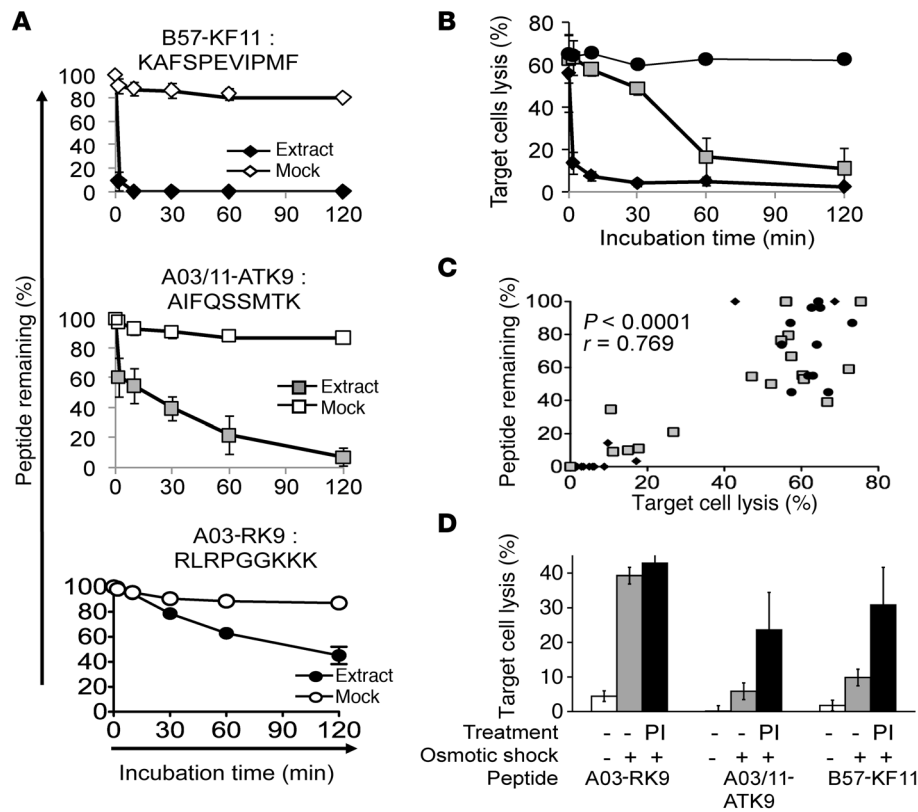
Figure 1
Intracellular HIV epitope stability is variable and degradation is correlated with reduced epitope antigenicity. (**A**) HLA-B57–restricted KF11 (diamonds), HLA-A03/11–restricted ATK9 (squares), and HLA-A03–restricted RK9 epitope (circles) were degraded in equal amounts of PBMC extracts (black or gray symbols) or buffer (open symbols). Aliquots of degradation products were analyzed and quantified by HPLC profile analysis after 2, 10, 30, 60, and 120 minutes. 100% represents the amount of peptide detected by HPLC at time 0 calculated as the surface under the peptide peak (2,487,757, 1,227,535, 1,614,506 for KF11, ATK9, and RK9, respectively). (**B**) Aliquots of purified degradation products were used to pulse HLA-matched ^{51}Cr-labeled B cells. CTL responses against A03-RK9 (circles), A03/11-ATK9 (squares), and B57-KF11 (diamonds) were assessed by ^{51}Cr release assay. (**C**) The percentage of peptide remaining at each degradation time point (same symbols as in **A**) is plotted versus the percentage of cell lysis for each experiment. Comparison by Spearman test is indicated. (**D**) Peptides A03-RK9, A03/A11-ATK9, or B57-KF11 were introduced by osmotic shock into HLA-A03$^+$ or -B57$^+$ cells that were pretreated or not with protease inhibitors (PI) and used as targets in a cytolysis assay with A03-RK9–specific or B57-KF11–specific CTL clones. Cells were stained for cell death markers annexin (V-PE, 7-ADD) 1–4 hours after osmotic shock (6.69% dead cells for untreated cells; 7.96% for peptide-loaded cells; average difference over 3 experiments, 0.84% ± 0.6%). Data represent the mean ± SD of 3 independent experiments.

step involved in antigenic peptide production and presentation, namely cytosolic stability of oligopeptides, and demonstrate that changes in intracellular stability of antigenic peptides are predictable and affect CTL recognition.

Results

Measurement of intracellular stability of HIV epitopes in primary cells. In order to test the cytosolic stability of a large number of HIV-derived peptides in a relevant model, we developed an in vitro assay using the cytosol of healthy human PBMCs that was further validated by measurements of endogenous peptide stability and presentation to HIV-specific CTLs (Figure 1).

Highly purified peptides were incubated for 2 hours in the presence or absence of PBMC cytosol (Supplemental Figure 1; supplemental material available online with this article; doi:10.1172/JCI44932DS1). The amount of peptide remaining over time in cytosolic extracts was measured by reverse-phase HPLC (RP-HPLC) profile analysis, where each peak defined by its elution time repre-

sents one peptide, and the surface area under the peak is proportional to the amount of peptide. The degradation of the peptide results in reduction of its peak and the appearance of additional peaks corresponding to truncated peptides (Supplemental Figure 2A). A value of 100% was assigned to the amount of input peptide present at time 0, and the amount of peptides remaining was calculated at each time point (Supplemental Figure 2, B and C, and Figure 1A). We first measured the cytosolic stability of 3 optimally defined HIV epitopes that elicit frequent CTL responses in HIV-infected persons: HLA-B57–restricted KF11 (KAFSPEVIPMF, aa 30–40 in Gag p24), HLA-A03/11–restricted ATK9 (AIFQSSMTK, aa 158–166 in reverse transcriptase of HIV-1 polymerase), and HLA-A03–restricted RK9 (RLRPGGKKK, aa 20–28 in p17 Gag) (10), incubated in the presence or absence of PBMC cytosol (Figure 1A). Peptide KF11 was rapidly degraded in the presence of PBMC cytosol, with no intact peptide remaining after a 2-minute incubation, while 91% of input peptide was detected in the absence of PBMC extract (the half-life of the peptide calculated during a

shorter degradation is 13 seconds). The rapid degradation of this 9-mer is in accordance with the half-life measurements of similarly sized peptides microinjected into cells (3, 9). Degradation of A03/11-ATK9 proceeded more slowly, with 61% of the input peptide remaining after 2 minutes and with complete degradation reached only after a 2-hour incubation with extracts (half-life, 2.1 minutes). In marked contrast to KF11, the RK9 peptide appeared to be extremely stable in PBMC cytosol, with 96% of input peptide remaining after a 2-minute incubation and 45% remaining after 2 hours (half-life, 90 minutes). The different degradation rates of KF11, ATK9, and RK9 suggest that the intracellular stability of short HIV peptides is highly variable.

Since these HIV peptides correspond to HLA-restricted epitopes of optimal length to bind HLA molecules and elicit CD8+ T cell responses, their degradation into peptides that are too short to bind HLA molecules should correlate with decreased antigenic potential. In order to measure the antigenicity of peptides present in the digestion mix over 2 hours, peptides were purified at each indicated time point and used to pulse HLA-matched B cells used as targets in a ^{51}Cr release assay with CTLs specific for B57-KF11, A03/11-ATK9, or A03-RK9 (Figure 1B). All 3 peptides have similar avidity for their respective CTLs (as in ref. 11), such that changes in antigenicity are similarly likely due to effects of peptide degradation. In accordance with peptide degradation measured by RP-HPLC, the antigenicity of the digestion products isolated over 2 hours variably decreased for all 3 peptides. The antigenicity of KF11 degradation products decreased sharply, by 87%, in 10 minutes and was abolished at 30 minutes, in agreement with rapid peptide degradation. The antigenicity of ATK9 degradation products decreased slowly during the first 30 minutes, resulting in a 23% reduction in 30 minutes, consistent with an intermediate intracellular stability. In contrast, RK9 peptide products remained highly antigenic throughout this time course, with a reduction of only 2% in target cell lysis for degradation products generated in 2 hours. This result is in accordance with the high intracellular stability of the peptide observed by HPLC profile analysis. We compared the amount of peptide remaining over the 2-hour degradation as measured by RP-HPLC with the corresponding antigenicity based on two independent experiments using extracts from different donors (Figure 1C). We found a strong association between the two values (P < 0.0001, r = 0.769, Spearman test), indicating that peptide degradation as measured by HPLC accurately corresponded to a loss of antigenicity as measured in a CTL cytolysis assay.

We next confirmed that the variable rates of peptide degradation we detected in vitro corresponded with natural phenomena occurring within cells, and examined whether these differences affected CTL recognition. To assess endogenous intracellular peptide stability independently of upstream steps of protein degradation, we introduced peptides into cells by osmotic shock as described previously (11) and monitored the capacity of cells to be recognized and killed by epitope-specific CTLs (Figure 1D). We chose one stable and two unstable peptides (A03-RK9, A03/11-ATK9, and B57-KF11, respectively) with equivalent functional avidity of the corresponding CTL clones (ref. 11 and data not shown). Cells that received peptide RK9 were sensitive to killing by RK9-specific CTL clones after peptide transfer in the presence or absence of protease inhibitor (39.3% vs. 42.9% lysis, respectively), suggesting that the peptide had not been degraded inside cells before presentation. In contrast, cells osmotically loaded with ATK9 or KF11 displayed limited lysis by epitope-specific CTLs (5.9% and 9.8% lysis). Pre-

treatment of target cells with protease inhibitors prior to peptide transfection rendered them sensitive to lysis by epitope-specific CTLs (23.7% vs. 5.9% lysis for ATK9 and 30.9% vs. 9.8% lysis for KF11, Figure 1D). By comparing the lysis of transfected cells with that of cells pulsed with increasing amounts of KF11, we observed that preincubation of cells with protease inhibitors increased the peptide presentation by 5.2-fold for ATK9 and 3.6-fold for KF11 (in contrast to 1.2-fold for A03-RK9). Although RK9 was 2- to 2.7-fold more efficiently loaded into cells than ATK9 or KF11 (calculated as the ratio of percent lysis of uploaded cells in the presence of inhibitors to the amount of exogenously pulsed peptides required to reach the same percent lysis), the increase in ATK9 and KF11 presentation after peptidase inhibition suggests that ATK9 and KF11 were rapidly degraded in the cells, thus limiting epitope presentation to CTLs.

To overcome differences in peptide uptake, we compared the endogenous presentation of RK9 and ATK9 processed from the same protein, p17, appended with RWEKI-ATK9 (RWEKI is the natural flanking sequence of RK9) (Supplemental Figure 3). We had shown that RK9 and ATK9 can be produced in cytosol from RWEKI-RK9 or RWEKI-ATK9 (11); thus, the main possible difference in epitope production and presentation will originate from their cytosolic stability. HLA-03 cells transfected with p17-RWEKI-ATK9 were efficiently lysed by RK9-specific CTLs and poorly by ATK9-specific CTLs (37.8% and 5.4%, respectively) (Supplemental Figure 3A). Similarly, the presentation of RK9 and ATK9 from RT appended with WKGSP-RK9 (WKGSP is the natural ATK9 flanking sequence) led to efficient RK9-specific response and poor ATK9-specific response (32.7% and 4.1%, respectively) (Supplemental Figure 3B). Measurement of epitope presentation showed a 7.9- and 5.1-fold increase of RK9 over AKT9 from p17-RWEKI-AKT9 and RT-WKGSP-RK9, respectively (Supplemental Figure 3C). Thus, RK9 is better processed and presented than ATK9, even when expressed from the same protein and flanked by the same sequence, regardless of its position in the protein. Together the results indicate that in the context of either osmotic loading of 9-mers into cells or endogenous expression of hybrid protein, higher intracellular stability of RK9 contributes to better presentation of that epitope to CTLs.

The intracellular stability of optimal HIV epitopes is highly variable. We set out to compare the stability of 166 HIV-derived peptides (8–11 aa) that were identified as optimal epitopes in large cohorts of persons infected with subtype B HIV-1 (10, 12) (Supplemental Table 2). Optimal epitopes are the shortest peptides yielding the strongest HLA-restricted and epitope-specific CTL response measured by IFN-γ ELISpot or ^{51}Cr release assay. Epitope sequences corresponded to the consensus subtype B virus of 2007 in the Los Alamos HIV database (12). The peptides covered 50%–90% of the total number of finely mapped HIV epitopes in each HIV protein, with the exception of 4 Vpu epitopes, for which the HPLC degradation profiles were not interpretable (Figure 2A). Epitopes were distributed across 75 HLA types (50%–100% of the total number of finely mapped HIV epitopes per restricting HLA). We observed that the cytosolic stability of HIV-derived peptides was highly variable, with 0%–100% peptide remaining after a 2-minute incubation in PBMC cytosol. A similar wide range of peptide stability was observed after a 10- or 30-minute incubation in PBMC extracts from several healthy donors. In order to assign a value to peptide stability covering a wide range of half-lives, we calculated a stability rate using nonlinear regression (one-phase exponential decay) of the degradation
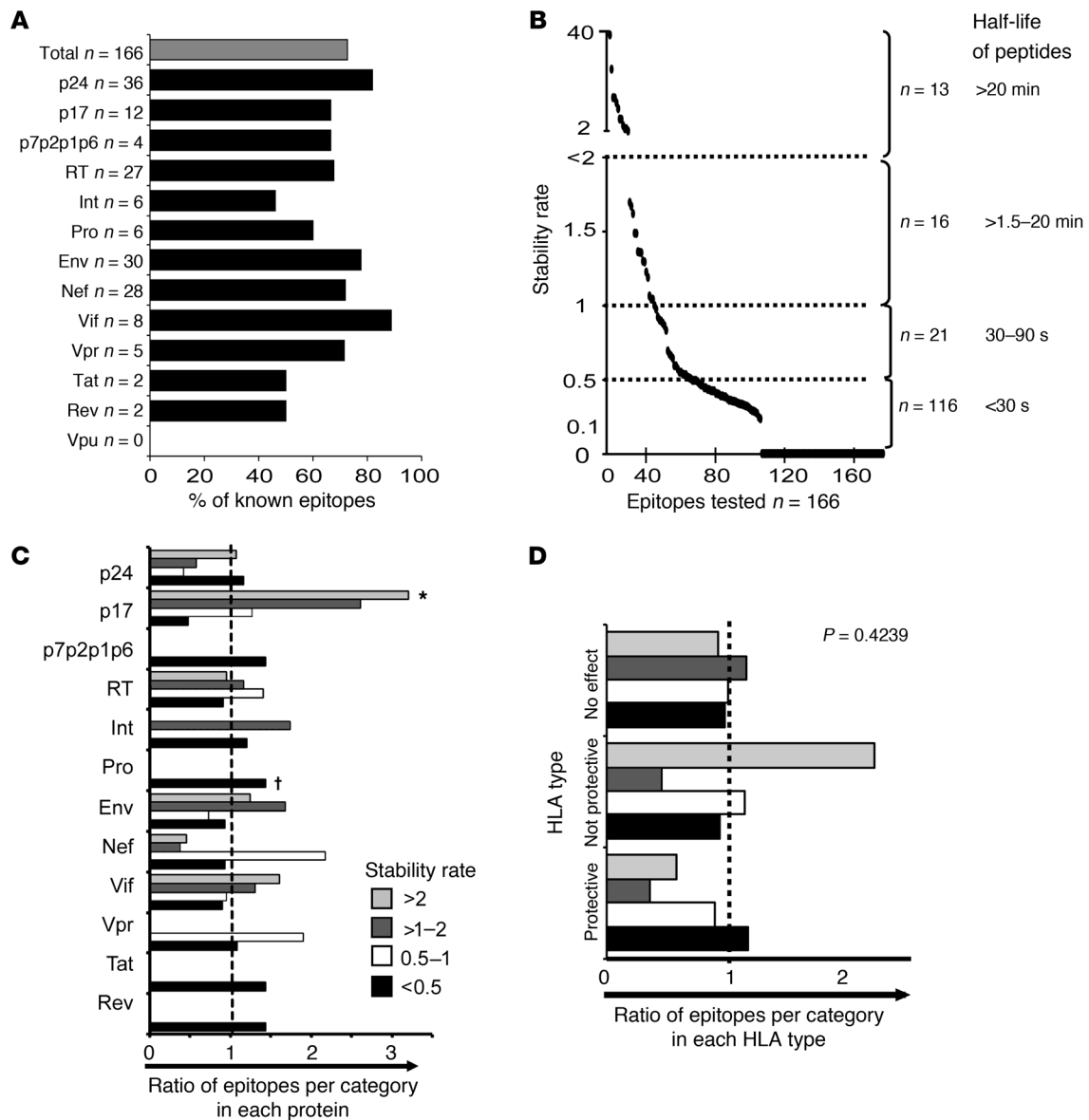
Figure 2
The cytosolic stability of HIV epitopes is highly variable. (**A**) Distribution of 166 optimal HIV epitopes (gray bar) across HIV proteins (black bars). (**B**) The stability rate of 166 epitopes was calculated by a nonlinear regression (one-phase exponential decay) of the degradation profile obtained over a 30-minute incubation in PBMC cytosol (average of >3 independent experiments with extracts from different donors). Four stability groups of epitopes were identified according to their stability rates (<0.1, 0.1–0.5, >0.5–1, >1–2, and >2) and corresponding half-life brackets (<30 seconds, 30–90 seconds, >1.5–20 minutes, >20 minutes). (**C**) Ratio between the percentage of epitopes in each protein in each stability bracket and the percentage of epitopes in this bracket for all proteins. *$P = 0.016$ and †$P = 0.0129$ for p17- and Protease-derived (Pro) peptides; Mann-Whitney U test. (**D**) Distribution of peptide stability rates according to restricting HLA alleles (protective: HLA-B27, -B51, -B57; not protective: HLA-B08 and -B35; no effect: all other 68 HLAs). Ratio between the percentage of epitopes in each stability bracket for each HLA group and the percentage of epitopes in each stability bracket for all HLAs tested. $P = 0.4239$ for the overall comparison between the 3 groups of HLAs (Mann-Whitney U test). The comparison between protective and nonprotective HLA alleles showed $P = 0.3667$ for unstable peptides (stability rate, <0.5), $P = 0.1669$ for intermediate peptides (0.5–1), $P = 0.1777$ for peptides with stability rates >1–2 minutes, and $P = 0.1612$ for the most stable peptides (>2).

profile over 30 minutes for an average of 3–5 experiments with different donors, and confirmed it with up to 12 different donors for the most stable epitopes. The intracellular stability rates of HIV epitopes were extremely variable, ranging from 39 to 0.0037 (Figure 2B). A majority of epitopes ($n = 116$, 69.9%) had stability rates of 0.0037 to 0.5, corresponding to peptide half-lives ranging from 10

to 30 seconds. This result is in accordance with previous reports in other models showing the short half-life of microinjected peptides (9) or minigenes encoding epitopes into cell lines (3). Many HIV-derived peptides ($n = 50$) displayed greater stability than those previously described — 37 peptides (22.3%) ranged between 0.5 and 2 (half-lives, 90 seconds–20 minutes), while 13 peptides (7.8%) dem-

Table 1

Stability motifs identified by computational analysis
of 166 HIV sequences

Stability features	Weight
Medium in end 3	1.6399
Positive in end 2	1.6163
Medium, positive in end 3	1.5648
Medium, large in end 3	1.5222
Medium, charged in end 3	1.4407
Aliphatic, large in begin 3	1.4172
Aromatic, medium in epitope	1.4159
Charged in end 2	1.3791
Medium, polar in end 2	1.3346
Large, buried in begin 3	1.2783
Charged, large in middle 3	1.251
Buried, large in begin 3	1.2137
Polar, aliphatic in middle 2	1.203
Cyclic, aliphatic in end 3	1.1971
Negative, large in middle 3	1.1868
Aliphatic, hydrophobic in middle 3	1.1744
Medium, charged in end 2	1.1472
Medium, positive in end 2	1.1472
L in middle 2	1.1296
Cyclic, aliphatic in end 2	1.122
Polar, positive in end 3	1.1045
Aliphatic, aliphatic in middle 3	1.0913
Aliphatic, polar in middle 2	1.0783
V in begin 3	1.067
Large, buried in begin 2	1.0413

Peptides were divided into 3 areas: first 2 or 3 aa (begin 2 or 3), last 2 or 3 aa (end 2 or 3), and middle of the epitope. Each feature was given a weight according to its impact on peptide half-lives. The most significant stability features (greater than +1) or unstable motifs (less than –1) are listed.

onstrated unusual stability rates of greater than 2–39 (half-lives, >20 minutes). This study identified a notably wide range of sensitivity to intracellular degradation among HIV peptides and provides the first identification to our knowledge of very long-lived peptides in the cytosol.

Clustering of stable peptides in HIV proteome. We analyzed the distribution of stable and unstable epitopes across HIV proteins and restricting HLA alleles (Figure 2C). In order to account for the variable number of epitopes located in each HIV protein, we calculated the ratio between the percentage of epitopes in each stability rate bracket for a given protein and the percentage of epitopes in the same stability rate bracket for all HIV proteins, highlighting by a ratio of greater than 1 the enrichment for a HIV protein of peptides within a stability rate category. We observed that Gag p24 and Gag p17, Env, and Vif were enriched in stable epitopes, whereas Nef, Protease, RT, Vpr, Tat, and Rev were enriched for unstable epitopes. Gag p17 displayed the highest proportion of epitopes with stability rate greater than 2 (half-lives, 2.5–120 minutes). A multiple comparisons analysis showed a significant difference in the distribution of stable and unstable epitopes between Gag p17 ($P = 0.016$) and Protease ($P = 0.0129$). Enrichment in stable and unstable epitopes did not segregate with conservation or variability of HIV at the protein level. The distribution of epitope stability among HLA alleles showed a significantly higher percentage of stable epitopes for HLA-A03–restricted epitopes ($P = 0.0001$, Mann-Whitney U test). Since the HLA-A03 molecule binds pep-

tides with a positively charged C-terminal anchor, this suggests that specific motifs may contribute to peptide stability. However, why peptides restricted by HLA-A03 would be more stable than those restricted by the closely related HLA-A11 is not clear. The distribution of epitopes did not differ significantly among protective (HLA-B57, -B27, and -B51), nonprotective (HLA-B35 and -B08), and neutral HLA alleles (all 68 other HLA alleles) ($P = 0.4239$), although a trend toward enrichment in stable epitopes ($P = 0.1612$) was seen for nonprotective alleles (Figure 2D). Stable or unstable peptides correspond to epitopes covering a wide range of MHC-I binding affinities; since cytosolic degradation of peptides occurs prior to binding to MHC-I, it was expected that peptide stability and MHC-I binding affinity would not correlate.

Cytosolic stability of HIV peptides is defined by specific motifs. We next sought to identify factors defining the intracellular stability of HIV epitopes, hypothesizing that specific sequences within peptides may confer susceptibility or resistance to hydrolysis by intracellular peptidases. We performed a computational analysis of all 166 epitopes to identify motifs distinguishing stable or unstable peptides, defined as those with greater than or less than 0.5 stability rate (half-life less than or greater than 30 seconds), respectively. Each peptide sequence was divided into several areas: the first 2 and 3 aa, the central area of 5 or 6 aa, and last 2 and 3 aa (Tables 1 and 2). The motifs within each area of peptides included size, charge, or hydrophobicity of single aa or pairs or triplets of aa (see Supplemental Table 1 for aa features). We built a predictive model that mapped features of a peptide to the probability that the peptide was stable. We used an L1-regularized logistic regression model, due to its simplicity and better performance in prediction of CTL epitopes (13) (Supplemental Figure 4). We tested and validated the model using 10-fold cross-validation (14). First, the 166 peptides were split randomly into 10 groups. Nine groups (90% of the data) were used to train the model and identify features linked to peptide stability rate. The model was then used to predict — based on the presence of motifs — the stability rate of each peptide in the remaining 10% of the dataset. The analysis was performed 10 times with permutation of the 90/10 split of the 166 peptides, thus yielding predicted stability rate values for the entire set of peptides. Peptide stability predictions and experimental values of the 166 peptides strongly correlated ($P < 0.0001$; Supplemental Figure 4). The model, constructed using all the data, identified 1,628 features for predicting peptide stability. Besides the identification of motifs, we associated with each feature a weight, such that features with higher weights had a greater influence on the probability of stability or instability. Positive (negative) weights corresponded to features positively (negatively) correlated with stability. Features with the highest-magnitude weights are shown in Tables 1 and 2. To illustrate the differences in the number and type of motifs among peptides, we calculated a stability score as the sum of the weights of all stability and instability motifs. As expected for a stable peptide, A03-RK9 (90-minute half-life) had a high score of +11.5, whereas unstable B57-KF11 (13-second half-life) had a low score of –18 (Figure 3).

Cytosolic peptide stability is predictable and can be manipulated. In order to further demonstrate that intracellular peptide stability is determined by motifs, and to validate the utility of our algorithm, we aimed to alter peptide stability through mutations in motifs identified by the model. First we attempted to destabilize naturally stable peptide A03-RK9 by reducing the number of stability motifs and increasing the number of instability

Table 2
Instability motifs identified by computational analysis
of 166 HIV sequences

Instability features	Weight
Polar, small in epitope	−1.7695
Buried, buried in end 3	−1.6743
Polar, hydrophobic in end 3	−1.5956
Buried, buried in end 2	−1.4454
Polar, hydrophobic in end 2	−1.3984
Cyclic, large in middle 2	−1.3936
Aromatic, large in epitope	−1.3607
Buried, hydrophobic in middle 2	−1.3528
Large, buried in end 3	−1.3428
Large, small in begin 3	−1.2993
Charged in begin 3	−1.2893
Buried, buried in epitope	−1.285
Hydrophobic, hydrophobic in middle 2	−1.2597
Small, positive in epitope	−1.2344
Large, small in epitope	−1.2211
Medium, hydrophobic in end 2	−1.2128
Medium, buried in end 2	−1.1975
Cyclic, large in epitope	−1.1833
Negative in begin 3	−1.1833
KA in epitope	−1.1451
Charged, hydrophobic in epitope	−1.1206
Hydrophobic, buried in middle 2	−1.1094
Small, large in end 3	−1.1076
Hydrophobic, aromatic in epitope	−1.092
Cyclic, large in begin 3	−1.0857

Peptides were divided into 3 areas: first 2 or 3 aa (begin 2 or 3), last 2 or 3 aa (end 2 or 3), and middle of the epitope. Each feature was given a weight according to its impact on peptide half-lives. The most significant instability motifs (less than −1) are listed.

motifs. For instance, two mutations in A03-RK9 (K7W, K8Y) destroyed two stability motifs and added two instability motifs, resulting in a –6.8 stability score (Figure 3). Twenty-five mutant RK9 peptides were designed through 1- to 7-aa substitutions at various positions and combinations (Figure 4A). We measured the cytosolic stability of each mutant and compared it with that of WT RK9. Remarkably, some mutations, such as A03-RK9 (K7W, K8Y), reduced the stability rate of RK9 from 12.9 to 0.24 (a 54-fold reduction), leading to a dramatic decrease in peptide half-life (90 minutes to 52 seconds), thus demonstrating that epitope stability is driven by specific motifs. Furthermore, we observed that identical mutations inserted at different positions within this peptide had variable effects on stability. For example, a tyrosine substitution at position 3 reduced the RK9 stability rate to 0.65 (half-life 40 seconds) (Figure 4A), while the same substitution at position 8 increased peptide stability rate to 36.5 (half-life, >120 minutes) (Figure 4B). These results demonstrate that both motifs and their location in the sequence contribute to peptide stability. Next we aimed to augment the half-lives of peptides through substitutions of destabilizing motifs into epitope sequences as illustrated in Figure 3 and Figure 4B for unstable B57-KF11. Such mutations were engineered for two naturally unstable epitopes, HLA-B57-KF11 and HLA-B27-KK10 (KRWIILGLNK, aa 131–140 in Gag p24), as well as that of a stable epitope (HLA-A03-RK9). We introduced 4 substitutions into KF11, KK10, or RK9 to generate 11 variant peptides (Fig-

ure 4B). These changes in sequence resulted in 1.1- to 13.5-fold increases in peptide stability rate (Figure 4B). Additionally, the experimental stability rates of all 36 variant peptides and those predicted by the algorithm showed a very strong correlation ($P = 0.0006$; Figure 4C), further validating the capacity of the algorithm to estimate peptide stability rates, since these variant peptides were not used to build the model. These results show that peptide intracellular half-life is defined by specific motifs at particular locations, can be altered through mutations, and can be predicted by this new sequence-based algorithm. This algorithm is available at http://research.microsoft.com/en-us/um/redmond/projects/MSCompBio/StabilityPrediction/.

Peptide resistance or sensitivity to cytosolic degradation are independent mechanisms. Thus far, our study assessed the stability of peptides independently of each other and using a defined ratio of peptide to cytosol. However, degradation rates may differ according to the peptide/cytosol ratio and the presence of stable or unstable peptides within the same cytosol. We examined the degradation of stable or unstable peptides in the presence of increasing amounts of PBMC cytosol as well as in the presence or absence of excess peptides (Supplemental Figure 5).

A stable peptide was stable in the presence of 2.5–80 µg of PBMC cytosol, suggesting that stability of this peptide was likely due to a lack of susceptibility to cleavage, rather than merely a limited amount of cytosolic activity. An unstable peptide remained unstable unless the cytosol amount was decreased by 16-fold. As expected for short peptides (5, 6, 15), degradation was not mediated by the proteasome or TPPII; however, we observed a role for TOP and cysteine or serine proteases, whereby preincubation of extracts with specific inhibitors increased peptide half-lives by 5- to 100-fold (data not shown). We tested whether the lack of degradation of more stable peptides might be due to a direct inhibition of cellular peptidases. The stability rate of stable or unstable peptides was largely unaffected by the presence or absence of the other peptide (80%–110% of half-life without a second peptide) (Supplemental Figure 5). These results suggest that stable peptides do not prevent the degradation of unstable peptides, nor do they inhibit the activity of cytosolic peptidases. Thus, stability of certain peptides and degradation of others are independent properties.

Cytosolic stability of some HIV peptides is mediated by chaperone complexes. We investigated whether cellular chaperones such as Hsp90 (4, 16) may protect HIV peptides from degradation in primary cells. PBMC cytosolic extracts were immunodepleted of Hsp90, histone deacetylase 6 (HDAC6; a binding partner of Hsp90), or irrelevant GAPDH or mock-depleted with species-matched IgG (Supplemental Figure 6). Equal amounts of extracts were used to degrade various HIV epitopes. The half-life of some peptides, such as B42-TL10 (TPGPGVRYPL, aa 128–137 in Nef), was reduced following Hsp90 or HDAC6 depletion (from 19 to 5–6 minutes), whereas that of B40-SL9 (SEGATPQDL, aa 44–52 in Nef) was unchanged (Figure 5A). Changes in peptide stability were presented as the percentage of peptide stability rate determined using mock-depleted extracts (Figure 5B). Hsp90 depletion reduced the stability rate of B42-TL10 and A03/11-ATK9 to 39% and 51% of control, respectively. Hsp90 has many binding partners, including HDAC6, which is involved in the formation of aggresomes of ubiquitinated proteins (17, 18). The depletion of HDAC6 in cytosol reduced the stability of B42-TL10 and A03/11-ATK9 to 44% and 55% of control conditions. Additionally, depletion of both Hsp90 and HDAC6 had additive effects on reducing B42-TL10 and A03/11-ATK9 stability rates to
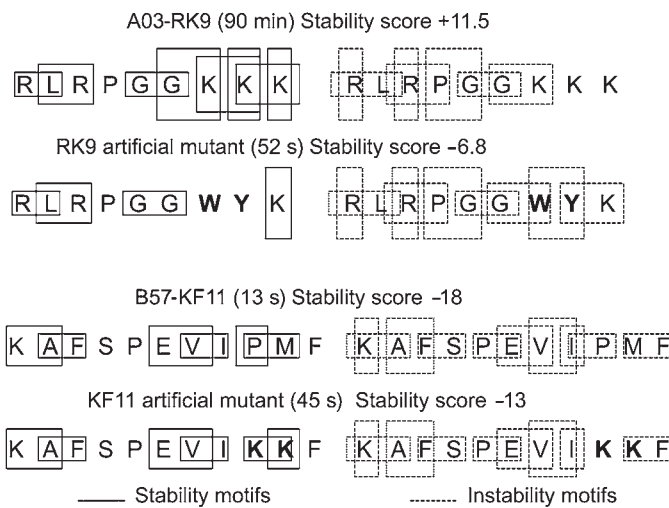
A03-RK9 (90 min) Stability score +11.5

RK9 artificial mutant (52 s) Stability score –6.8

B57-KF11 (13 s) Stability score –18

KF11 artificial mutant (45 s) Stability score –13

——— Stability motifs   ·········· Instability motifs

Figure 3
Identification of stability and instability motifs in HIV sequences and artificial mutants. Examples of stability (solid boxes) and instability (dashed boxes) motifs in stable A03-RK9 and unstable B57-KF11 and artificial mutants of each epitope designed to test the algorithm (cytosolic half-lives in parenthesis). A stability score was calculated for each peptide as the sum of all stability and instability motif weights listed in Tables 1 and 2.

26% and 38% of control conditions (Figure 5B). These results suggest that a complex involving Hsp90 and HDAC6 contributed to protection of these peptides from degradation. In order to determine which partner is involved in peptide protection, we incubated PBMC extracts with inhibitors of Hsp90 (17AAG blocks ATP binding to Hsp90 and its chaperone function), HDAC6 (trichostatin A [TSA] interferes with HDAC6 acetylation function), cysteine protease (E64), or DMSO prior to peptide degradation (Figure 5C). These inhibitors did not affect the half-life of peptide B40-SL9 (not altered by Hsp90/HDAC6 depletion). In contrast, the stability rate of B42-TL10, a peptide protected from degradation by Hsp90/HDAC6, was decreased in the presence of Hsp90 inhibitor (60% of that of control conditions; half-life, 5 minutes) and strongly decreased in the presence of HDAC6 inhibitor (14%; half-life, 1.8 minute) or a combination of Hsp90 and HDAC6 inhibitors (9%). These results suggest that protection from cytosolic degradation of some HIV peptides may occur through direct interaction with HDAC6 or through an HDAC6 partner requiring intact HDAC6 function, but not through direct binding to Hsp90 (or through ATP-independent function of Hsp90). Other peptides, such as B4001-SL9 and B35-PIY9 (NPPIPVGEIY, aa 122–130 in p24), displayed equivalent half-lives in the presence or absence of these chaperones (76% to 94% stability rate of control conditions) or inhibitors. Their relative stability may be a direct result of the lack of suitable cleavage sites for cytosolic peptidases or indicate the involvement of other cellular partners.

Naturally occurring HLA-restricted mutations reducing the intracellular stability of HIV epitopes lead to immune escape. CD8+ T cell responses exert a strong selective pressure on HIV, and numerous HLA-associated intraepitopic mutations have been identified in large cohorts of HIV-infected persons (19–21). We examined whether HLA-restricted mutations within epitopes may affect the intracellular stability of peptides and thus limit the amount of peptide available for loading onto HLA molecules and recognition by CTLs.

We selected two epitopes known to mutate early in HIV infection, B08-FL8 (FLKEKGGL, aa 90–97 in Nef) and B57-TW10 (TSTLQEQIGW, aa 108-117 in Gag p24) (22, 23), and for which the variant peptide was predicted by the algorithm to display reduced stability (Figure 6A). We first compared the half-life of B08-FL8 epitope and the two most frequent B08-associated mutations observed in acute/early subtype B infection (B08-FL8 K5N and K5M, where residue 5 has been mutated into N and M, respectively) (21, 23). Mutation 5N in B8-FL8 slightly reduced the peptide half-life, by 18% (1.8 vs 2.2 minutes for the WT), whereas mutation 5M markedly reduced the peptide half-life, by 91%, to 12 seconds. A similar analysis was done for B57-TW10 in Gag p24 and its variants. The first TW10 mutation to appear in acute infection, T3N, reduces binding to HLA-B57, while the double mutation T3N-G9A or T3N-G9D is associated with decreased viral fitness (22, 24). We observed that WT HLA-B57-TW10 and the T3N peptide were stable (31 and 33 minutes, respectively), whereas the half-life of the double mutant T3N-G9A was decreased by 92% to 45 seconds (corresponding to a difference in stability rate of 80%, 2.2 to 0.4521). Single mutants B57-TW10 G9D and B57-TW10 G9A also displayed decreased half-lives (1.4 and 1.7 minutes, respectively), suggesting that residues 3 and 9 both contributed to TW10 peptide stability, and/or that each mutation creates intraepitopic cleavage sites. In order to test directly whether mutations reducing peptide intracellular stability affected the amount of epitope displayed at the cell surface and CTL recognition, we infected HLA-B57+ cells at equal MOI with VSV-G–pseudotyped HIV-1 NL4-3–derived strains containing WT TW10 or TW10 G9D. Infected cells were used as targets in a killing assay with CTL clones specific for either B57-TW10 or B57-KF11, a neighboring epitope in p24 (Figure 6B). Cells infected by WT or G9D virus were equally recognized and killed by B57-KF11 CTLs (30.9% vs. 35.9% lysis, respectively), indicating equivalent infection rates and expression and degradation of p24 from the two viruses. In contrast, B57-TW10–specific CTLs were 8.75-fold less efficient at killing cells infected with NL4-3 G9D compared with WT (5.5% vs. 48.1% lysis, respectively). Since B57-TW10–specific CTLs equally recognized HLA-B57+ cells exogenously pulsed with increasing amounts of either WT TW10 or TW10 G9D epitope (Figure 6C), these results suggest that the two peptides have similar binding to HLA and elicit comparable responses by the CTLs used, but that TW10 G9D epitope is less efficiently processed and presented than WT TW10. By comparing percent specific lysis of infected cells with that of cells pulsed with increasing amounts of TW10 or TW10 G9D, we calculated that the G9D mutation reduced by 6.4-fold the amount of antigenic peptide displayed at the cell surface for recognition by B57-TW10 specific CTLs. Additionally, the in vitro degradation of p24 peptides containing either TW10 or TW10 G9D showed efficient production of TW10 but not of TW10 G9D, in accordance with the quick degradation of TW10 G9D in cytosolic extracts (data not shown). We monitored TW10, TW10 G9D, and KF11 epitope presentation to CTLs at 1–4 days after infection (Supplemental Figure 7). CTL activation was measured as the percentage of cells expressing CD8 and the degranulation marker CD107a (Supplemental Figure 7A). In the presence of cells infected with WT virus, CTL degranulation peaked at day 2 after infection for both KF11- and TW10-specific CTLs (16% and 28.9% CD8+CD107a+ for
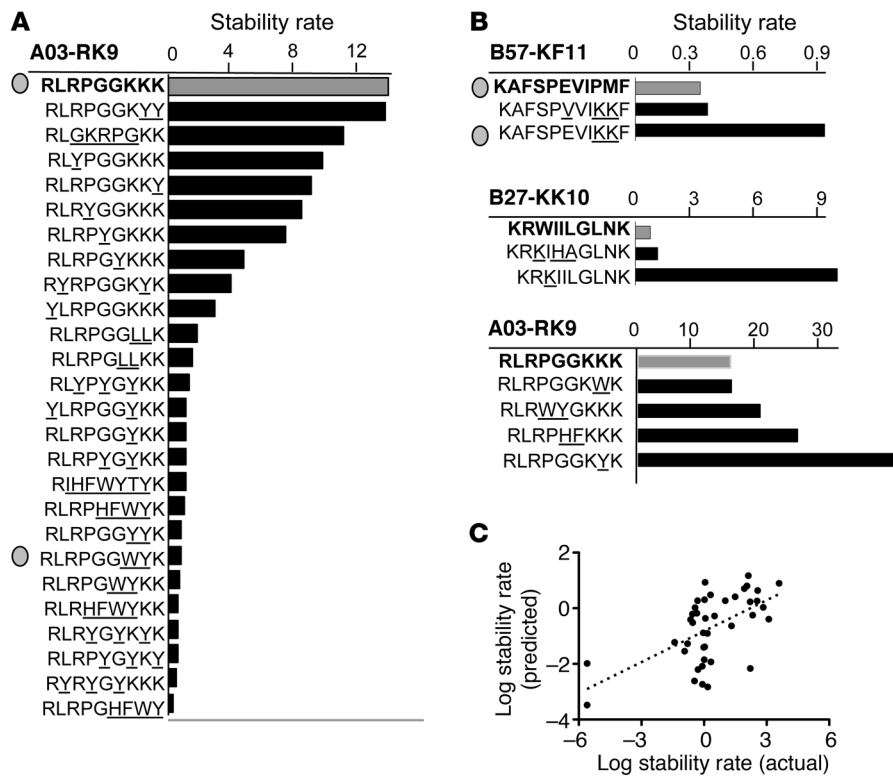
Figure 4
Cytosolic peptide stability can be modulated through mutations of motifs. (**A**) Stability rates of 25 mutants (black bars) of A03-RK9 epitope (gray). One to 7 mutations (underlined) in the RK9 sequence reduced the number of stability motifs. Peptides described in Figure 3 are indicated with a gray dot. (**B**) Stability motifs were added in B57-KF11, B27-KK10, and A03-RK9, and stability rates of all mutants were experimentally measured. Data represent the mean of at least 3 independent experiments. (**C**) Correlation between the logarithmic values of stability rates of the 36 mutants determined experimentally (actual half-life) and the stability rates predicted by the algorithm trained with stability rates of consensus sequences of HIV-derived epitopes (predicted stability rates). P = 0.0006 (Spearman test).

KF11 and TW10, respectively) and decreased to baseline at day 4, in agreement with single-round infection kinetics (Supplemental Figure 7B). In the presence of cells infected with HIV G9D, the kinetics of KF11 activation was similar to that of WT. However, the amount of CD107a^{+} TW10 CTLs remained very low between days 1 and 4 (maximum of 1.18% double-positive TW10 CTLs), suggesting that TW10 G9D was not efficiently presented for several days after infection. Together these data suggest that the G9D mutation in HLA-B57–restricted TW10 reduces the production of TW10 peptide due to higher intracellular degradation rates, which limits the amount of epitope available for recognition by CTLs and reduces killing of infected cells by TW10-specific CTLs.

We then asked to what extent HLA-restricted mutations inside epitopes affect cytosolic peptide stability. We measured the cytosolic stability rates of 12 WT peptides and their 25 corresponding HLA-restricted mutants, which were described in cohorts of acutely or chronically HIV-infected persons (Table 3). Of 25 mutants, 9 (36% of tested mutants) mutants dramatically reduced peptide half-life by 67%–99.6% and 7 (28% of tested mutations) reduced peptide stability rates by 50%–55%, while 3 (12%) had less of an impact (18%–42% reduction). Four mutations (16%) had almost no effect on peptide stability. Two mutations increased peptide stability, but these mutations at the C-terminal residues prevent binding of the peptide to HLA-A03 and are therefore not presented (ref. 25 and data not shown). Altogether 64% of mutations strongly reduced intracellular peptide stability by more than 50%. A 95.5% reduction in peptide half-life abolished CTL killing (88.5% reduction) despite equivalent high avidity of the two peptides (Figure 6). It is likely that mutations reducing peptide stability by 50%–99% (specifically for peptides with lower binding affinity to MHC-I than the strong binder TW10) may have a dramatic effect on

CTL recognition, although this remains to be demonstrated. HLA-restricted intraepitopic mutations decreasing intracellular peptide stability constitute what is to our knowledge a novel mechanism of immune escape in HIV infection.

Discussion

Despite the identification of multiple peptidases involved in epitope processing, there is limited knowledge about either sequences in the protein substrate that will ultimately become antigenic or the efficiency of production and presentation of antigenic peptides to CD8^{+} T cells. Cytosolic proteins are degraded into long fragments further trimmed into short peptides. The competition between complete degradation of these peptides and loading onto MHC-I complexes likely plays a key role in defining the amount of peptides available for display at the cell surface. Because short peptides could interfere with cellular functions, it has been postulated that cytosolic short peptides are rapidly degraded (3, 4). However, the impact of intracellular peptide stability on pathogen-derived epitope presentation and the adaptive immune response is not known.

Our study provides an extensive analysis of HIV-derived peptide half-lives in primary cells. By testing 166 HIV peptides, we identified 50 peptides that displayed much longer half-lives than those previously reported (3, 4). A computational model that incorporated data from 166 HIV peptides identified multiple motifs located throughout a peptide sequence that enhance or inhibit degradation of peptides. Mutation of identified stability motifs rendered peptides more sensitive to degradation, and conversely, mutations of identified instability sequences toward stable motifs resulted in slower degradation. Completely artificial peptides made of mainly stable or unstable motifs displayed concordant long or short cytosolic half-lives, further validating the computational identifi-
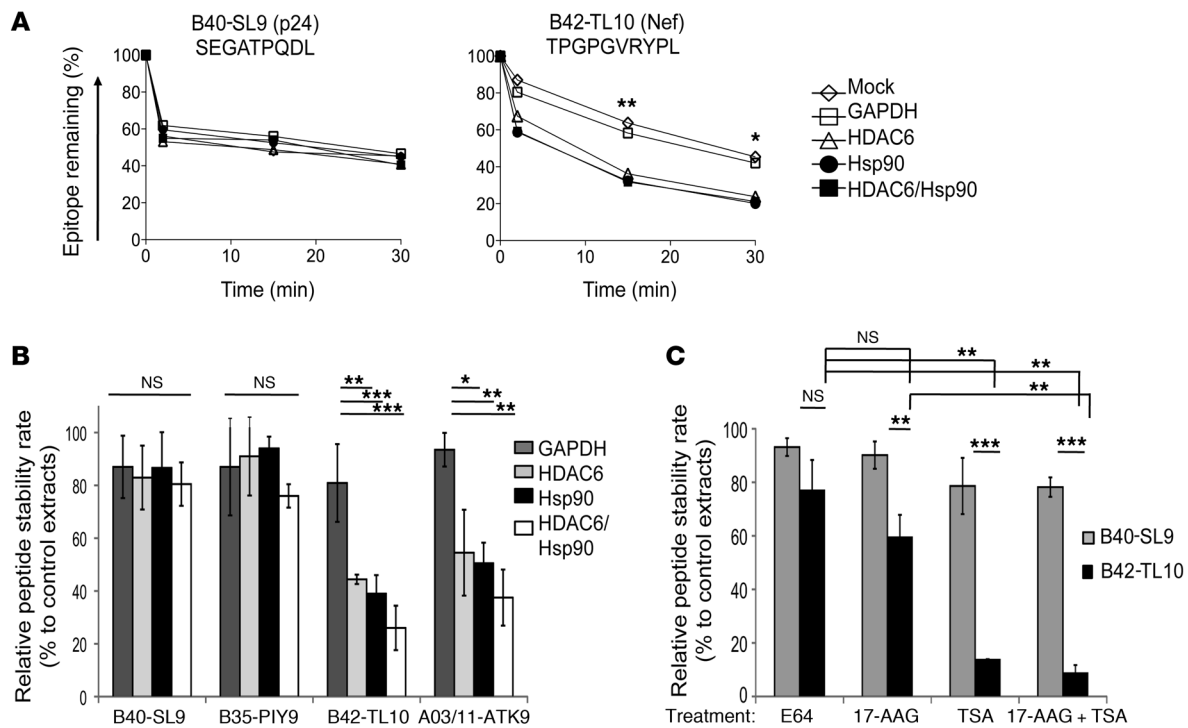
Figure 5
The cytosolic stability of some HIV peptides involves Hsp90-HDAC6 complexes. (**A**) B40-SL9 peptide (aa 44–52 in Nef) or B42-TL10 (aa 128–37) was degraded in cytosol either mock depleted or depleted of GAPDH, HDAC6, Hsp90, or HDAC6 plus Hsp90. The amount of peptide remaining was measured over 30 minutes. (**B**) PBMC extracts were preincubated in the presence of cysteine protease, Hsp90, or HDAC6 inhibitors (E64, 17AAG, or TSA, respectively) or in the absence of any inhibitor, prior to degradation of B40-SL9 or B42-TL10. The stability rate of each peptide in each condition was calculated as a percentage of that of the peptide in the absence of inhibitors. Data represent the mean ± SD of 3 independent experiments with extracts from 3 different donors. *$P < 0.05$, **$P < 0.01$. (**C**) Degradation in depleted extracts was performed for B40-SL9 (dark gray), B35-PIY9 (PPIPVGEIY, aa 122–130 in p24) (light gray), B42-TL10 (black), and A03/11-ATK9 (white), and peptide stability rates in each condition were calculated as the percent stability rate in mock-depleted extracts. *$P < 0.05$, **$P < 0.01$, ***$P < 0.001$, 2-way ANOVA with Bonferroni post-test.
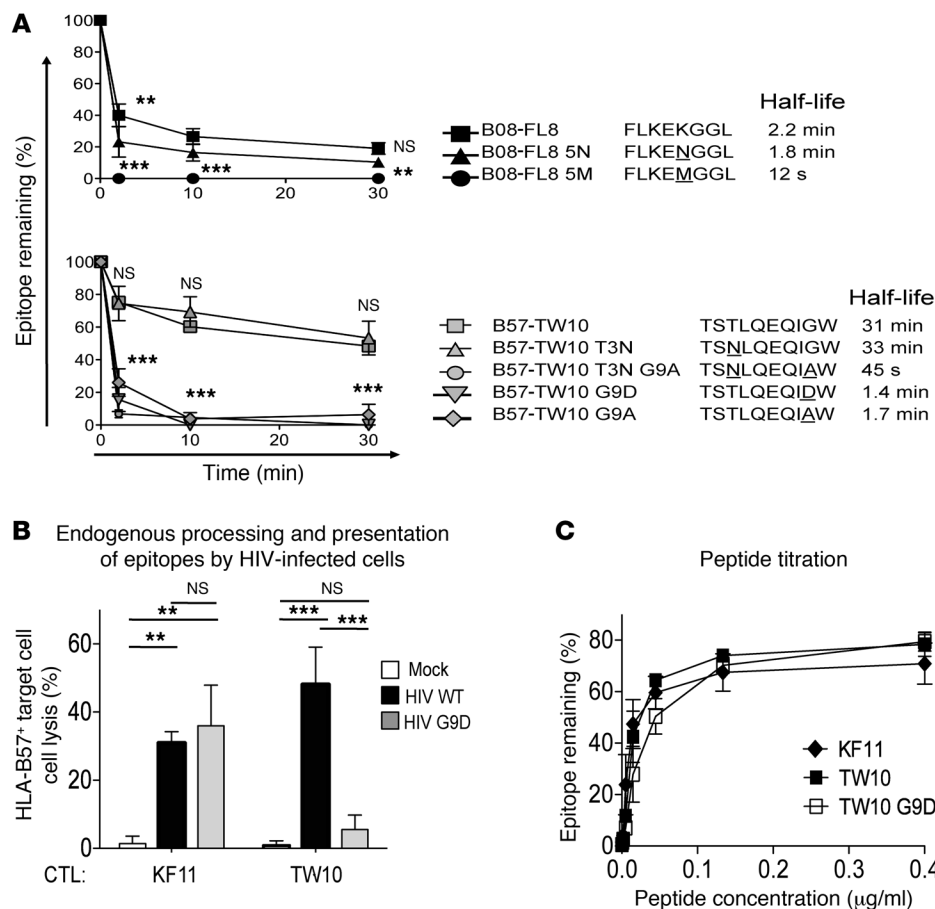
cation of stability motifs (data not shown). Several peptides derived from ovalbumin, EBV, and influenza A displayed highly variable half-lives (from <30 seconds to >30 minutes; data not shown). This suggests that peptide stability is strongly affected by motifs and is variable across epitopes derived from multiple pathogens.

The wide range of short peptide half-lives and search for motifs defining stability were established using cytosolic extracts purified from human PBMCs. One limitation of this approach is that it may abolish the compartmentalization of proteases or other cytosolic proteins that might affect peptide stability. However, the variability of peptide half-lives and its subsequent impact on presentation to CTLs were confirmed in live cells using 3 different approaches (osmotic loading of peptides, transfection of vectors expressing HIV proteins, and HIV infection), providing strong support for this in vitro approach.

One mechanism that may contribute to peptide stability is a transient association with cellular chaperones. We show that a complex involving Hsp90 and HDAC6 protects some HIV peptides from degradation, although only functional HDAC6 — but not the ATP-dependent function of Hsp90 — appears to be involved. The role of HDAC6 in protecting oligopeptides from complete degradation along with its contribution to the formation of aggregosomes of ubiquitinated proteins (17) defines HDAC6 as a player not only in

protein degradation, but also in epitope presentation. Whether interaction between HDAC6 and peptide is direct remains to be investigated. Some HIV-derived peptides remained stable in the absence of Hsp90 or HDAC6, suggesting that additional mechanisms may alter the rate of peptide degradation. Since peptides can circulate between cytosol and nucleus (9), one cannot rule out protection of some peptides by other chaperones or histones. Protection may also be intrinsic to the peptide sequence. Multiple charges in peptides such as A03-RK9 (RLRPGGKKK) may prevent interaction with peptidases, or specific motifs may lead to aggregations of peptides in pools, as suggested for an influenza peptide in mouse cells (4), although the isolation of such pools of stable peptides remains to be achieved. Particular peptide conformations such as proline-rich regions may not fit well into the catalytic sites of proteases and thereby spare these sequences from degradation. It is also possible that some oligopeptides may not contain cleavage motifs for cytosolic peptidases. Finally, the relative number, accessibility, and affinity of each type of motif for chaperones or peptidases are likely to define the cytosolic stability of peptides and the amount of peptide available for downstream steps of epitope processing and presentation.

The amount of MHC-I–epitope complexes required to prime or activate CTL responses is not known and likely varies depending on the binding affinity of the peptide for MHC-I and the

Figure 6
Natural mutations occurring during HIV infection affect cytosolic peptide stability and CTL recognition. (**A**) B57-TW10 and HLA-B57–restricted mutants T3N (gray triangles), T3N-G9A, G9D, and G9A were degraded for 30 minutes in PBMC cytosol. The amount of peptide remaining and peptide half-lives are indicated. Similar experiments were performed with WT B08-FL8 and with B08-FL8 mutants 5N and 5M. For unstable peptides, the half-lives were determined during a 10-minute degradation. **$P < 0.01$, ***$P < 0.001$, NS or no symbol: not significant; comparison between peptide degradation by 2-way ANOVA with Bonferroni post-test between WT and each mutant peptide. (**B**) HLA-B57 cells were infected with NL4-3 (WT, black bars) or NL4-3 with G9D mutation in TW10 (gray bars) or no virus (Mock, white bars). Cells were used as targets in a killing assay with B57-KF11– or B57-TW10–specific CTLs. **$P < 0.01$, ***$P < 0.001$, 2-way ANOVA. (**C**) HLA-B57+ cells were pulsed with increasing amounts of B57-KF11, B57-TW10, or B57-TW10 G9D and used as target in a killing assay with B57-KF11–specific or B57-TW10–specific CTLs. In **A**–**C**, data represent the mean ± SD of 3 independent experiments.

TCR. Our results reveal a critical role for a motif-dependent cytosolic peptide stability or sensitivity to degradation in defining the amount of epitope displayed to CTLs.

If increased cytosolic stability allows the display of more peptide-HLA complexes, this early step of antigen processing may contribute to efficient activation of CD8+ T cells. Accordingly, endogenous processing and presentation of unstable B57-TW10 G9D led to an 8.8-fold reduction in CTL-mediated killing of infected cells, corresponding to a 6.4-fold reduction in TW10 G9D peptide presentation compared with that of WT TW10. Similarly, endogenous presentation of stable A03-RK9 and unstable A03/11 ATK9 or B57-KF11 after osmotic loading of the peptides into cells revealed that increased intracellular degradation of A03/11-ATK9 or B57-KF11 leads to reduced activation of the corresponding CTLs despite equivalent functional avidity of the two peptides for the respective clones. Additional evidence for the importance of cytosolic peptide stability for CTL recognition comes from the identification of 16 HLA-associated mutations

that reduced intracellular peptide stability by more than 50%. For one mutant, for which intracellular half-life was reduced by 95%, CTL-mediated killing of infected cells was reduced by 88.5% despite equivalent functional avidity of the WT and mutated peptide, identifying what we believe to be a novel mechanism of viral escape impairing CTL recognition. Thus, viral evolution may drive immune escape through multiple mechanisms: mutations that reduce binding to HLA or to the TCR (19, 21), mutations in flanking regions that prevent the complete processing of epitopes (26), and mutations that increase cytosolic peptide degradation, as reported here.

Prior steps of protein degradation leading to the production of oligopeptides are critical to epitope display. We had previously shown that motifs flanking epitopes contribute to the efficiency of production of HIV epitopes (11). HLA-A03-RK9 epitope is both produced rapidly (11) and highly stable compared with other HLA-A03–restricted epitopes such as A03/11-ATK9 in RT (Figure 1A). Together, early and efficient production of A03-RK9 and

Table 3
HLA-restricted intraepitopic mutations affect intracellular peptide stability

Peptide name	Sequence	Half-life	% Reduction (−) or increase (+) compared with WT stability	Comments and references about mutations
B57-TW10 (p24)	TSTLQEQIGW	31 min		
TW10 T3N	TSNLQEQIGW	33 min	+6	22, 32; 88.5% reduction of
TW10 T3NG9A	TSNLQEQIAW	50 s	−97.3	CTL-mediated lysis (Figure 6B; Supplemental Figure 7)
TW10 G9D	TSTLQEQIDW	1.4 min	−95.5	
TW10 G9A	TSTLQEQIAW	1.7 min	−94.5	
B08-FL8 (Nef)	FLKEKGGL	2.2 min		33
FL8 K5M	FLKEMGGL	12 s	−91	Figure 6A
FL8 K5N	FLKENGGL	1.8 min	−18	
B27-KK10 (p24)	KRWIILGLNK	1.5 min		32, 34
KK10 R2G	KGWIILGLNK	26 s	−71	
KK10 R2K/L6M	KKWIIMGLNK	38 s	−74	
KK10 L6M	KRWIIMGLNK	45 s	−50	
KK10 R2K/L6M/N8H	KRWIIMGLHK	15 s	−83.3	
A02-SL9 (p17)	SLYNTVATL	1.1 min		32
SL9-T8V	SLYNTVAVL	<30 s	>−55	
SL9-Y3F	SLFNTVATL	<30 s	>−55	
SL9-V6I	SLYNTIATL	<30 s	>−55	
SL9-V6I/T8V	SLYNTIAVL	<30 s	>−55	
SL9-Y3F/V6I	SLFNTIATL	<30 s	>−55	
A02-AL9 (Vpr)	AIIRILQQL	45 s		33
AL9 I5T	AIIRTLQQL	20 s	−56	
B44-AW11 (p24)	AEQASQDVKNW	1.2 min		32
AW11 D7E	AEQASQEVKNW	25 s	−79	
B08-WM8 (Nef)	WPTVRERM	1.7 min		33
WM8 P2Y	WYTVRERM	1.1 min	−35	
B51-EI9 (Vpr)	EAVRHFPRI	1.1 min		
EI9 (Vpr) I9T	EAVRHFPRT	22 s	−67	33
EI9 (Vpr) I9A	EAVRHFPRA	38 s	−42	
B35-VY8 (Nef)	VPLRPMTY	30 s		12, 33
VY8 Y8F	VPLRPMTF	30 s	0	
B07-FL9 (Nef)	FPVTPQVPL	1.4 min		12, 33
FL9 V3K	FPKTPQVPL	1.35 min	−4	
B57-HW9 (Nef) WT	HTQGYFPDW	30 s		33
HW9 H1N	NTQGYFPDW	30 s	0	
A03 RK9 (p17)	RLRPGGKKK	90 min		25, 32
RK9 K9Q	RLRPGGKKQ	>120 min	Increase	
RK9 K9T	RLRPGGKKT	>120 min	Increase	

WT sequences are from HXB2. Average of 3 experiments performed with cytosolic extracts from 3 different donors.

resistance to cytosolic degradation may result in rapid presentation of relatively high amounts of RK9 peptides and contribute to the immunodominance status of the corresponding CTL response in acute HIV infection (27). Although there is no direct correlation between peptide stability and immunodominance hierarchy for the 166 peptides tested, it is worth noting that 3 of the 12 most stable epitopes (half-lives, >20 minutes) correspond to immunodominant CTL responses in acute HIV infection. Our results suggest that stable epitopes may be presented in larger amounts. It is unclear how much peptide is needed for optimal T cell activation for a given CTL response or whether too much peptide (or a longer display of peptides) may lead to overactivation of T cells.

Finally, the identification of a factor involved in epitope presentation, namely cytosolic stability of short peptides, is of the utmost interest for immunogen design. HIV-specific CTL responses have been observed to display unequal antiviral capacity (28), and immunodominant responses are not always protective (29). Future T cell–based immunogens should specifically produce epitopes that elicit particularly protective responses. In addition to altering peptide liberation, as we previously proposed (11), modulation of cytosolic peptide stability offers a unique way to regulate epitope presentation to reduce activation of nonprotective CTL responses and favor the presentation of epitopes eliciting protective responses.

Methods

Peptides and reagents. Highly purified peptides (>98% pure) were purchased from the Massachusetts General Hospital peptide core facility or from Bio-Synthesis. All chemicals were purchased from Sigma-Aldrich and antibodies from Santa Cruz Biotechnology Inc.

Study participants and primary cells. Buffy coats from anonymous volunteers were purchased from Massachusetts General Hospital. The use of buffy coats was approved under protocol 2005P001218 by the Partners Human Research Committee, Boston, Massachusetts, USA.

In vitro epitope degradation and antigenicity assay. PBMC cytosol was purified and checked for cytosolic antigen processing activities and lack of lysosomal activities as shown in Supplemental Figure 1 and refs. 11, 30. Eight nanomoles of peptides was degraded with 40 μg PBMC cytosol (11, 30). Peptides present in the digestion mix were identified and quantified by RP-HPLC. In order to measure antigenicity of the degradation products, peptides present in the digestion mix were purified and diluted in RPMI without serum (R+), and pH was readjusted to 7.4. Cells were pulsed with 0.02 μg/ml digestion products without serum and used as targets in killing assays with epitope-specific CTL clones at a 4:1 ratio. Percent lysis of HLA-matched B cells pulsed with degradation products was compared with that of cells pulsed with undigested long peptides or optimal epitopes at concentrations ranging from 0 to 0.4 μg/ml (11, 30).

Endogenous epitope stability assay. B cells were transfected with peptides by osmotic loading, a technique adapted from ref. 31 we previously used (11). 2×10^6 cells were incubated at 37°C for 10 minutes with 30–100 nM peptides in 500 μl hyperosmotic buffer followed by 3 minutes in 15 ml hypotonic buffer (60% R+ in water). Cells were resuspended in 500 μl R+ and used as targets in a ^{51}Cr release assay. The osmotic shock did not induce cell death or modify Cr uptake. When indicated, cells were preincubated with 500 μM AEBSF for 30 minutes before transfection and throughout the experiment. Upon addition of the CTLs, the concentrations of the drugs were reduced by half and did not affect CTL killing capacity (data not shown).

Endogenous HIV epitope processing and presentation to CTL. HIV-1 G9D is derived from NL4-3 and contains a G9D mutation in HLA-B57–restricted TW10 epitope (residue 248 in Gag) and was a gift from Mark A. Brockman, Simon Fraser University, Burnaby, British Columbia, Canada (24). VSV-G–pseudotyped viral stocks were prepared by cotransfection of 293T cells with proviral DNA with a CMV-VSV-G plasmid and titrated as previously described (24). HLA-B57+ CD4+ T or B cells were infected with either WT or mutated HIV-1 for 6 hours at an MOI of 0.1. Mock- or HIV-infected cells were used 24 hours later as targets in a ^{51}Cr release assay with epitope-specific CTL clones (4:1 ratio). Endogenous processing and presentation of epitopes were also assessed in transiently transfected cells as previously described (11).

CTL degranulation assay. CTL activation was measured by the expression of the degranulation marker CD107a in CD8+ T cells after incubation with uninfected cells or cells infected with HIV WT or HIV G9D. CTLs and target cells were mixed at a 4:1 ratio. Cells were stimulated 2 hours with PMA (2.5 μg/ml) and ionomycin (0.5 μg/ml) as a positive control. After a 6-hour incubation with 5 μg/ml brefeldin A, 0.9 μg/ml of monensin (GolgiStop, BD), and CD107a-FITC antibody, cells were stained with CD8-PE antibody (pre-titrated volume; BD). Cells were fixed and acquired on a FACSCalibur. Data were analyzed using FlowJo software.

Cytosol immunodepletion. PBMC cytosol was precleared with species-matched serum and protein A/G slurry for 20 minutes at 4°C. Cytosol (100 μg) was incubated for 4 hours at 4°C with antibodies specific for each protein of interest. Buffer-washed protein A/G slurry was added for 30 minutes. Supernatant corresponds to immunodepleted cytosol. Immunodepletion efficiency was checked by Western blotting against the target protein and actin as loading control. Equal amounts of extracts were used for epitope degradation assays.

Statistics. Empirical data were analyzed using GraphPad Prism version 5, including nonparametric correlations by Spearman test with 2-tailed P values, comparisons between groups by 2-tailed Mann-Whitney U tests, 2-way ANOVA with Bonferroni post-test. P values less than 0.05 were considered statistically significant.

Address correspondence to: Sylvie Le Gall, Ragon Institute of MGH, MIT and Harvard, Massachusetts General Hospital, Harvard Medical School, CNY Bldg 149, 13th Street, Boston, Massachusetts 02129, USA. Phone: 617.726.1406; Fax: 617.726.5411; E-mail: sylvie_legall@hms.harvard.edu.

1. Princiotta MF, et al. Quantitating protein synthesis, degradation, and endogenous antigen processing. *Immunity.* 2003;18(3):343–354.
2. Goldberg A, Cascio P, Saric T, Rock KL. The importance of the proteasome and subsequent proteolytic steps in the generation of antigenic peptides. *Mol Immunol.* 2002;39(3-4):147–164.
3. Herberts CA, et al. Cutting edge: HLA-B27 acquires many N-terminal dibasic peptides: coupling cytosolic peptide stability to antigen presentation. *J Immunol.* 2006;176(5):2697–2701.
4. Lev A, et al. The exception that reinforces the rule: crosspriming by cytosolic peptides that escape degradation. *Immunity.* 2008;28(6):787–798.
5. Saric T, Graef CI, Goldberg AL. Pathway for degradation of peptides generated by proteasomes: a key role for thimet oligopeptidase and other metallopeptidases. *J Biol Chem.* 2004;279(45):46723–46732.
6. York IA, et al. The cytosolic endopeptidase, thimet oligopeptidase, destroys antigenic peptides and limits the extent of MHC class I antigen presentation. *Immunity.* 2003;18(3):429–440.
7. Kawahara M, York IA, Hearn A, Farfan D, Rock KL. Analysis of the role of tripeptidyl peptidase II in MHC class I antigen presentation in vivo. *J Immunol.* 2009;183(10):6069–6077.
8. Reits E, et al. A major role for TPPII in trimming proteasomal degradation products for MHC class I antigen presentation. *Immunity.* 2004;20(4):495–506.
9. Reits EA, et al. Peptide diffusion, protection, and degradation in nuclear and cytoplasmic compartments before antigen presentation by MHC-I. *Immunity.* 2003;18(1):97–108.
10. Korber BTM, et al. *HIV Molecular Immunology 2009.* Los Alamos, New Mexico, USA: Los Alamos National Laboratory, Theoretical Biology and Biophysics; 2008.
11. Le Gall S, Stamegna P, Walker BD. Portable flanking sequences modulate CTL epitope processing. *J Clin Invest.* 2007;117(11):3563–3575.
12. Frahm N, Baker B, Brander C. Identification and optimal definition of HIV-derived cytotoxic T lymphocyte (CTL) epitopes for the study of CTL escape, functional avidity and viral evolution. In: Korber BT, et al., eds. *HIV Molecular Immunology 2008.* Los Alamos, New Mexico, USA: Los Alamos National Laboratory, Theoretical Biology and Biophysics; 2008.
13. Heckerman D, Kadie C, Listgarten J. Leveraging information across HLA alleles/supertypes improves epitope prediction. *J Comput Biol.* 2007;14(6):736–746.
14. Tibshirani R. Regression shrinkage and selection via the Lasso. *J R Stat Soc Series B Stat Methodol.* 1996;58(1):267–288.
15. Saric T, Beninga J, Graef CI, Akopian T, Rock KL, Goldberg AL. Major histocompatibility complex class I-presented antigenic peptides are degraded in cytosolic extracts primarily by thimet oligopeptidase. *J Biol Chem.* 2001;276(39):36474–36481.
16. Kunisawa J, Shastri N. Hsp90alpha chaperones large C-terminally extended proteolytic intermediates in the MHC class I antigen processing pathway. *Immunity.* 2006;24(5):523–534.
17. Kawaguchi Y, Kovacs JJ, McLaurin A, Vance JM, Ito A, Yao TP. The deacetylase HDAC6 regulates aggresome formation and cell viability in response to misfolded protein stress. *Cell.* 2003;115(6):727–738.
18. Valenzuela-Fernandez A, Cabrero JR, Serrador JM,

Sanchez-Madrid F. HDAC6: a key regulator of cyto-skeleton, cell migration and cell-cell interactions. *Trends Cell Biol*. 2008;18(6):291–297.

19. Allen TM, et al. De novo generation of escape variant-specific CD8+ T-cell responses following cytotoxic T-lymphocyte escape in chronic human immunodeficiency virus type 1 infection. *J Virol*. 2005;79(20):12952–12960.

20. Jones NA, et al. Determinants of human immunodeficiency virus type 1 escape from the primary CD8+ cytotoxic T lymphocyte response. *J Exp Med*. 2004;200(10):1243–1256.

21. Price DA, et al. Positive selection of HIV–1 cytotoxic T lymphocyte escape variants during primary infection. *Proc Natl Acad Sci U S A*. 1997;94(5):1890–1895.

22. Brockman MA, et al. Escape and compensation from early HLA-B57-mediated cytotoxic T-lymphocyte pressure on human immunodeficiency virus type 1 Gag alter capsid interactions with cyclophilin A. *J Virol*. 2007;81(22):12608–12618.

23. Brumme ZL, et al. Marked epitope- and allele-specific differences in rates of mutation in human immunodeficiency type 1 (HIV-1) Gag, Pol, and Nef cytotoxic T-lymphocyte epitopes in acute/early

HIV-1 infection. *J Virol*. 2008;82(18):9216–9227.

24. Miura T, et al. HLA-B57/B*5801 human immunodeficiency virus type 1 elite controllers select for rare gag variants associated with reduced viral replication capacity and strong cytotoxic T-lymphocyte recognition. *J Virol*. 2009;83(6):2743–2755.

25. Allen TM, et al. Selection, transmission, and reversion of an antigen-processing cytotoxic T-lymphocyte escape mutation in human immunodeficiency virus type 1 infection. *J Virol*. 2004;78(13):7069–7078.

26. Draenert R, et al. Immune selection for altered antigen processing leads to cytotoxic T lymphocyte escape in chronic HIV-1 infection. *J Exp Med*. 2004;199(7):905–915.

27. Yu XG, et al. Consistent patterns in the development and immunodominance of human immunodeficiency virus type 1 (HIV-1)-specific CD8+ T-cell responses following acute HIV-1 infection. *J Virol*. 2002;76(17):8690–8701.

28. Chen H, et al. Differential neutralization of human immunodeficiency virus (HIV) replication in autologous CD4 T cells by HIV-specific cytotoxic T lymphocytes. *J Virol*. 2009;83(7):3138–3149.

29. Frahm N, et al. Control of human immunodefi-

ciency virus replication by cytotoxic T lymphocytes targeting subdominant epitopes. *Nat Immunol*. 2006;7(2):173–178.

30. Lazaro E, et al. Differential HIV epitope processing in monocytes and CD4 T cells affects cytotoxic T lymphocyte recognition. *J Infect Dis*. 2009; 200(2):236–243.

31. Moore MW, Carbone FR, Bevan MJ. Introduction of soluble protein into the class I pathway of antigen processing and presentation. *Cell*. 1988; 54(6):777–785.

32. Brumme ZL, et al. Human leukocyte antigen-specific polymorphisms in HIV-1 Gag and their association with viral load in chronic untreated infection. *Aids*. 2008;22(11):1277–1286.

33. Brumme ZL, et al. Evidence of differential HLA class I-mediated viral evolution in functional and accessory/regulatory genes of HIV-1. *PLoS Pathog*. 2007;3(7):e94.

34. Schneidewind A, et al. Escape from the dominant HLA-B27-restricted cytotoxic T-lymphocyte response in Gag is associated with a dramatic reduction in human immunodeficiency virus type 1 replication. *J Virol*. 2007;81(22):12382–12393.